Journal of Computational Physics **154,** 266–283 (1999)
Article ID jcph.1999.6313, available online at http://www.idealibrary.com on IDEAL®

Well-posed Perfectly Matched Layers for Advective Acoustics

S. Abarbanel,* D. Gottlieb,† and J. S. Hesthaven†

**Department of Applied Mathematics, Tel Aviv University, Tel Aviv, Israel; †Division of Applied Mathematics, Brown University, Box F, Providence, Rhode Island 02912*
E-mail: saul@math.tau.ac.il, dig@cfm.brown.edu, jansh@cfm.brown.edu

Received October 26, 1998; revised May 26, 1999

Using a mathematical framework originally developed for the development of PML schemes in computational electromagnetics, we develop a set of strongly well-posed PML equations for the absorption of acoustic and vorticity waves in two-dimensional convective acoustics under the assumption of a spatially constant mean flow. A central piece in this development is the development of a variable transformation that conserves the dispersion relation of the physical space equations. The PML equations are given for layers being perpendicular to the direction of the mean flow as well as for layers being parallel to the mean flow. The efficacy of the PML scheme is illustrated by solving the equations of acoustics using a 4th order scheme, confirming the accuracy as well as stability of the proposed scheme.

Key Words: advective acoustics; absorbing boundary conditions.

1. INTRODUCTION

The ability to accurately simulate wave phenomena is important in several physical fields, e.g., electromagnetics, ambient as well as advective acoustics associated with a mean flow, elasticity, and seismology.

Due to limited computing resources the numerical simulations of such problems often must be confined to truncated domains much smaller than the physical space in which the wave phenomena take place. In such cases, numerical reflections of outgoing waves from the boundaries of the numerical domain can reenter the computational domain and eventually falsify the results. This artifact limits the overall order of accuracy of the algorithm used in the computation and becomes particularly troublesome in cases where higher order of accuracy is required due to mode resolution, storage availability, etc.

To deal with these types of problems local non-reflecting boundary conditions were derived for the wave equation by Engquist and Majda [1] and later by Bayliss and Turkel [2].

0021-9991/99 $30.00

Reviews of such techniques can be found in [3, 4]. In practice, however, their effectiveness is limited. The notion of perfectly matched absorbing layers (PML) was introduced in the context of computational electromagnetics (CEM) by Berenger [5]. The idea behind PML is to attribute to the layers material properties that modify the original field equations so that the waves will decay in all directions of propagation in the layers. However, it has been shown by Abarbanel and Gottlieb [6] that the splitting technique, introduced by Berenger, results in a system of partial differential equations (PDEs) which are only weakly well-posed, i.e., they may become ill-posed under certain perturbations—an example of which is provided in [6]. Alternative methods to derive PML equations in CEM are to use physical considerations in establishing the absorbing source terms for the unsplit Maxwell's equations, as discussed in [7, 8]. An overview of such techniques can be found in [9]. These new equations are well-posed and yield reflection coefficients as small as obtained when using the Berenger PML equations. Yet another approach [10] is to derive the PML equations from purely mathematical considerations. This approach yields, in the CEM case, a family of PML equations that includes the equations in [8] as a special case.

It is straightforward to show that there is a one to one correspondence between the case of two-dimensional ambient acoustics (no mean flow) and transverse electromagnetic wave propagation. Hence the PML procedures of CEM may be applied directly to the case of ambient acoustics.

In this paper we consider the case of advected acoustics (non-vanishing mean flow) with the PML layers being normal and parallel to the mean flow. This problem was previously addressed by Hu [11] by generalizing Berenger's splitting technique to this case. However, as for the case of electromagnetics, Hesthaven [12] subsequently showed loss of strong well-posedness as a result of the splitting, hence explaining the problems of instability reported in [11]. Equivalent conclusions, although obtained through a different procedure, were reached in [13]. While alternatives, producing layers with PML like behavior, were proposed in [12] by artificially changing the flow Mach number continuously to zero within the PML layer and using the results from CEM, the construction of a well-posed PML method for general advective acoustics remains open.

It is to address this particular concern that we here propose to use an extension of the procedure, originally used in [10] to construct the PML equations for the case of electromagnetics by means of a mathematical procedure, to deal with the more complex case of advective acoustics.

In Section 2 we consider the two-dimensional equations of advected acoustic (linearized Euler equations) and present a coordinate transformation that allows for a more convenient derivation of the PML equations. Section 3 is devoted to a derivation of the PML equations for the absorbing layers surrounding the basic computational domain while Section 4 presents numerical results for a standard test problem, confirming the expected performance of the developed framework. Section 5 concludes with a few general remarks.

2. THE EQUATIONS OF ACOUSTICS

We consider the propagation of waves induced in a uniform two-dimensional subsonic flow, $(u_0, 0)$, of a compressible fluid, by small perturbations. This phenomenon is described by the linearized Euler equations for the perturbations of the density, ρ', and velocities, u'

and v', as

$$\frac{\partial \rho'}{\partial \bar{t}} + \bar{u}_0 \frac{\partial \rho'}{\partial \bar{x}} + \bar{\rho}_0 \frac{\partial u'}{\partial \bar{x}} + \rho_0 \frac{\partial v'}{\partial \bar{y}} = 0, \tag{2.1}$$

$$\frac{\partial u'}{\partial \bar{t}} + \bar{u}_0 \frac{\partial u'}{\partial \bar{x}} + \frac{\bar{c}_0^2}{\bar{\rho}_0} \frac{\partial \rho'}{\partial \bar{x}} = 0, \tag{2.2}$$

$$\frac{\partial v'}{\partial \bar{t}} + \bar{u}_0 \frac{\partial v'}{\partial \bar{x}} + \frac{\bar{c}_0^2}{\bar{\rho}_0} \frac{\partial \rho'}{\partial \bar{y}} = 0, \tag{2.3}$$

where we assumed isentropy of the flow, i.e., $\bar{p}_0 = \bar{p}_0(\bar{\rho}_0)$. The speed of sound, $\bar{c}_0$, is given by $\bar{c}_0^2 = d\bar{p}_0/d\bar{p}_0$ where $\bar{p}_0$, $\bar{\rho}_0$ are the unperturbed pressure and density of the flow. The dimensional time and distances are given by $\bar{t}$, $\bar{x}$, and $\bar{y}$.

We nondimensionalize this set of equations by using a reference length $\bar{x}_r = \bar{y}_r = L$ (usually related to the wavelength of the acoustic wave), and a reference time $\bar{t}_r = L/\bar{c}_0$. Similarly $\bar{\rho}_r = \bar{\rho}_0$ and $\bar{u}_r = \bar{v}_r = \bar{c}_0$. With $M = \bar{u}_0/\bar{c}_0$, the resulting set of dimensionless equations is

$$\frac{\partial \rho}{\partial t} + M \frac{\partial \rho}{\partial x} + \frac{\partial u}{\partial x} + \frac{\partial v}{\partial y} = 0, \tag{2.4}$$

$$\frac{\partial u}{\partial t} + M \frac{\partial u}{\partial x} + \frac{\partial \rho}{\partial x} = 0, \tag{2.5}$$

$$\frac{\partial v}{\partial t} + M \frac{\partial v}{\partial x} + \frac{\partial \rho}{\partial y} = 0, \tag{2.6}$$

where the prime $((\cdot)')$ has been dropped from the perturbation quantities. The case of ambient acoustics is obtained by letting the Mach number $M \to 0$. This case has been discussed by Hesthaven [12] and is known to correspond exactly to the case of two-dimensional electromagnetics. Hence, for $M = 0$, the solution of any smooth initial boundary value problem can be shown to be expressed as a superposition of plane waves on the form

$$\begin{pmatrix} \rho \\ u \\ v \end{pmatrix} \sim \begin{pmatrix} 1 \\ \alpha \\ \beta \end{pmatrix} e^{i\omega(t-\alpha x-\beta y)}, \tag{2.7}$$

with a dispersion relation of the form

$$\alpha^2 + \beta^2 = 1. \tag{2.8}$$

When $M \neq 0$, however, the resulting dispersion relation is much more complicated, and the analysis from the case of electromagnetics cannot easily be carried over to the case acoustic waves.

To overcome this difficulty we shall transform Eqs. (2.4)–(2.6) to a new set of coordinates, (ξ, η, τ), as

$$\xi = x, \tag{2.9}$$

$$\eta = \sqrt{1 - M^2}\, y = \gamma y, \tag{2.10}$$

$$\tau = Mx + \gamma^2 t. \tag{2.11}$$

This transformation is related to the one utilized in [2] although with stretching applied in y rather than in x as in [2]. As we shall see shortly, this difference is crucial.

The transformed equations take the form (with $\gamma = \sqrt{1 - M^2}$),

$$\frac{\partial v}{\partial \tau} + M\frac{\partial v}{\partial \xi} + \gamma\frac{\partial \rho}{\partial \eta} = 0, \tag{2.12}$$

$$\frac{\partial u}{\partial \tau} + \frac{\partial \rho}{\partial \xi} - \frac{M}{\gamma}\frac{\partial v}{\partial \eta} = 0, \tag{2.13}$$

$$\frac{\partial \rho}{\partial \tau} + \frac{\partial u}{\partial \xi} + \frac{1}{\gamma}\frac{\partial v}{\partial \eta} = 0. \tag{2.14}$$

Note that the order of the equations has been reorganized such that for $M = 0$ $(\gamma = 1)$, one recovers the two-dimensional transverse electric set of Maxwell's equations [9] through the simple transformation, $\rho \leftrightarrow H, u \leftrightarrow E_y, v \leftrightarrow -E_x$. This is done purely for convenience.

We shall seek plane wave solutions in the stretched space, (ξ, η, τ), of the form

$$\begin{pmatrix} v \\ u \\ \rho \end{pmatrix} = \begin{pmatrix} q_1 \\ q_2 \\ q_3 \end{pmatrix} e^{i\omega(\tau - B\eta - \lambda\xi)}. \tag{2.15}$$

For this ansatz to be a solution, λ must be the solvability eigenvalue of (2.12)–(2.14) after the substitution of (2.15). The three distinct eigenvalues are given as

$$\lambda_0 = 1/M, \tag{2.16}$$

$$\lambda_1 = \sqrt{1 - B^2} \triangleq A, \tag{2.17}$$

$$\lambda_2 = -\sqrt{1 - B^2} = -A, \tag{2.18}$$

with the three corresponding eigenvectors being

$$\mathbf{q}_0 = \begin{pmatrix} M \\ -\frac{M^2 B}{\gamma} \\ 0 \end{pmatrix}, \tag{2.19a}$$

$$\mathbf{q}_1 = \begin{pmatrix} B\gamma \\ A - M \\ 1 - MA \end{pmatrix}, \tag{2.19b}$$

$$\mathbf{q}_2 = \begin{pmatrix} B\gamma \\ -A - M \\ 1 + MA \end{pmatrix}. \tag{2.19c}$$

The λ_0-solution corresponds to the rightward moving vorticity wave whose amplitude tends to zero as $M \to 0$; see Eq. (2.19a). The λ_1 and λ_2 solutions represent the two counter-propagating acoustic waves moving to the right and left, respectively, in the (ξ, η)-plane. Note that because of the specific transformation $(x, y, t) \to (\xi, \eta, \tau)$ the eigenvalues $\lambda_1 =$

$A = -\lambda_2$ satisfy the standard dispersion relation

$$A^2 + B^2 = 1, \tag{2.20}$$

analogous to (2.8). The property is directly related to the particular transformation introduced in (2.9)–(2.11) and will, as we shall see shortly, play a central role in facilitating the subsequent analysis. Note also that in the physical plane the expression $A^2 + B^2 = 1$ does not constitute a dispersion relation.

3. CONSTRUCTION OF THE ABSORBING LAYER EQUATIONS

The set of Eqs. (2.12)–(2.14) is to be solved on a finite computational domain rather than the infinite domain on which the original analytical problem is set. We would like to ensure that waves leaving the domain are not reflected back as these could otherwise interact with the solution and eventually falsify it. The approach taken here is to surround the computational domain with finite width strips which must be defined such that the waves propagate into these absorbing layers without reflection and decay as they continue their travel inside these layers. Moreover, we shall require that these properties are independent of the frequency as well as the angle of incidence of the incoming wave. In the (x, y)-plane the typical arrangement is shown in Fig. 1.

In the following we shall discuss the developments of such layers and their properties in the ξ and η layers separately, recalling that (x, y, t) is related to (ξ, η, τ) through Eqs. (2.9)–(2.11).

3.1. *The Absorbing ξ-Layers*

We shall begin by demonstrating the construction of the PML equation for the layer, $-L_x - \delta_x \leq x \leq -L_x$ ($\xi \leq 0$ by normalization) into which only the counter-propagating sound wave can propagate. In other words, we consider the problem for $\lambda_2 = -A < 0$ in the setting of the transformed variables.

Inside the layer, $-\delta < \xi < 0$, we postulate that the solution is given as a superposition of decaying waves, each one being of the form

$$\begin{pmatrix} v \\ u \\ \rho \end{pmatrix} = \begin{bmatrix} (1+g)B\gamma \\ -(1+f)(A+M) \\ (1+h)(1+MA) \end{bmatrix} e^{i\omega(\tau + A\xi - B\eta)} e^{-A\int_{\xi<0}^{0} \sigma_x(z)dz}. \tag{3.1}$$

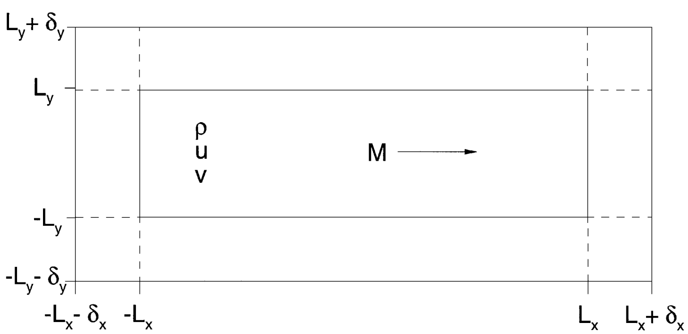

FIG. 1. Typical configuration in the (x, y)-plane of the absorbing layers.

The coefficients $g,\ f$, and h in the ansatz (3.1) are functions of ξ such that $g = f = h = 0$ for $\xi \geq 0$. The same is true for the positive quantity $\sigma_x(\xi)$. Substitution of (3.1) into (2.12)–(2.14) leads to a system of inhomogeneous PDEs

$$\frac{\partial v}{\partial \tau} + M\frac{\partial v}{\partial \xi} + \gamma\frac{\partial \rho}{\partial \eta} = \tilde{S}_1 e^{i\omega(\tau + A\xi - B\eta)} e^{-A\int_{\xi<0}^{0}\sigma_x(z)dz} = S_1, \tag{3.2}$$

$$\frac{\partial u}{\partial \tau} + \frac{\partial \rho}{\partial \xi} - \frac{M}{\gamma}\frac{\partial v}{\partial \eta} = \tilde{S}_2 e^{i\omega(\tau + A\xi - B\eta)} e^{-A\int_{\xi<0}^{0}\sigma_x(z)dz} = S_2, \tag{3.3}$$

$$\frac{\partial \rho}{\partial \tau} + \frac{\partial u}{\partial \xi} + \frac{1}{\gamma}\frac{\partial v}{\partial \eta} = \tilde{S}_3 e^{i\omega(\tau + A\xi - B\eta)} e^{-\int_{\xi<0}^{0}\sigma_x(z)dz} = S_3, \tag{3.4}$$

where the source terms, $\tilde{S}_j\,(j = 1, 2, 3)$, are given as

$$\tilde{S}_1 = B\gamma[i\omega(g - h) + Mg'] + B\gamma MA[(1 + g)(\sigma_x + i\omega) - (1 + h)i\omega], \tag{3.5}$$

$$\begin{aligned}\tilde{S}_2 = {} & [i\omega M(g - f) + h'] + A[-i\omega(1 + f) + (1 + h)(\sigma_x + i\omega) + Mh'] \\ & + A^2 M\,[(1 + h)(\sigma_x + i\omega) - i\omega(1 + g)]\,,\end{aligned} \tag{3.6}$$

$$\begin{aligned}\tilde{S}_3 = {} & [i\omega(h - g) - Mf'] + A[i\omega(1 + h)M - (1 + f)(\sigma_x + i\omega)M - f'] \\ & + A^2\,[i\omega(1 + g) - (1 + f)(\sigma_x + i\omega)]\,.\end{aligned} \tag{3.7}$$

We first note that with (3.5)–(3.7) as written here, the right hand side of the system (3.2)–(3.4) includes the frequency and dispersion parameters, (ω, A, and B), explicitly. Left in this form, the system (3.5)–(3.7) cannot describe an absorbing layer which is supposed to deal equally efficient with all frequencies, ω, and all directions of propagation, (A, B), of the incoming wave. It is clear, therefore, that $S_j\,(j = 1, 2, 3)$ must be cast in a form that precludes the explicit appearance of ω, A, and B in the system of Eqs. (3.2)–(3.4). As we shall see, this requirement will lead us to define new, and possibly unphysical, variables, as is the case for the PML methods in computational electromagnetics [10].

As a first condition we require the coefficients of A^2 in (3.6) and (3.7) to vanish as

$$M[(1 + h)(\sigma_x + i\omega) - i\omega(1 + g)] = 0, \tag{3.8}$$

and

$$[i\omega(1 + g) - (\sigma_x + i\omega)(1 + f)] = 0. \tag{3.9}$$

Since (3.8) must be valid for all $0 \leq M < 1$, it follows from (3.8) and (3.9) that

$$h = f. \tag{3.10}$$

As a second choice, we take $f = h = 0$, such that (3.6)–(3.7) become

$$\tilde{S}_2 = i\omega Mg + A\sigma_x, \tag{3.11}$$

$$\tilde{S}_3 = -i\omega g - AM\sigma_x. \tag{3.12}$$

Particularly simple $\tilde{S}_2$ and $\tilde{S}_3$ are recovered by setting

$$g = \frac{\sigma_x(\xi)}{i\omega}, \tag{3.13}$$

such that

$$S_2 = \sigma_x(M + A)e^{i\omega(\tau + A\xi - B\eta)}e^{-A\int_{\xi<0}^{0}\sigma_x(z)\,dz}, \tag{3.14}$$

$$S_3 = -\sigma_x(1 + AM)e^{i\omega(\tau + A\xi - B\eta)}e^{-A\int_{\xi<0}^{0}\sigma_x(z)\,dz}. \tag{3.15}$$

By referring to (2.19c) (the vector $\mathbf{q}_3$), we immediately see that (3.14)–(3.15) implies

$$S_2 = -\sigma_x u, \tag{3.16}$$

$$S_3 = -\sigma_x \rho. \tag{3.17}$$

Next we use $g = \sigma_x / i\omega$ and $h = 0$ in (3.5) and after somewhat lengthy algebraic manipulations we recover

$$\tilde{S}_1 = B\gamma\left[-\sigma_x\left(1 + \frac{\sigma_x}{i\omega}\right) + \frac{\sigma_x^2}{i\omega} + 2\sigma_x(1 + MA) + \frac{\sigma_x^2}{i\omega}MA + \frac{M\sigma_x'}{i\omega}\right]. \tag{3.18}$$

Unlike S_2 and S_3, S_1 cannot be cast only in terms of v, u, and ρ. On the other hand we still must require that S_1 not depend on ω, A, or B. To overcome this difficulty we define a number of new variables

$$P_x = \tilde{P}_x e^{i\omega(\tau + A\xi - B\eta)}e^{-\int_{\xi<0}^{0}\sigma_x(z)\,dz}, \tag{3.19}$$

$$Q_x = \tilde{Q}_x e^{i\omega(\tau + A\xi - B\eta)}e^{-\int_{\xi<0}^{0}\sigma_x(z)\,dz}, \tag{3.20}$$

$$R_x = \tilde{R}_x e^{i\omega(\tau + A\xi - B\eta)}e^{-\int_{\xi<0}^{0}\sigma_x(z)\,dz}, \tag{3.21}$$

where

$$\tilde{P}_x = \frac{B\gamma}{i\omega} = \frac{B\gamma}{i\omega}\left[\left(1 + \frac{\sigma_x}{i\omega}\right) - \frac{\sigma_x}{i\omega}\right], \tag{3.22}$$

and hence

$$\tilde{P}_x = \frac{v}{i\omega} - \sigma_x\frac{P_x}{i\omega}. \tag{3.23}$$

We also take

$$\tilde{Q}_x = B\gamma(1 + MA), \tag{3.24}$$

and

$$\tilde{R}_x = \frac{\tilde{Q}_x}{i\omega}. \tag{3.25}$$

Utilizing (3.23) we immediately recover (since $i\omega \leftrightarrow \partial/\partial\tau$) a differential equation for P

$$\frac{\partial P_x}{\partial \tau} = v - \sigma_x P_x. \tag{3.26}$$

From (3.24) we have

$$\begin{aligned}\frac{\partial Q_x}{\partial \tau} &= i\omega[B\gamma(1+MA)]e^{i\omega(\tau+A\xi-B\eta)}e^{-\int_{\xi<0}^{0}\sigma_x(z)dz}\\ &= i\omega B\gamma[(1+MA)]e^{i\omega(\tau+A\xi-B\eta)}e^{-\int_{\xi}^{0}\sigma_x(z)dz},\end{aligned}$$

and since $h = 0$, this is equivalent to (cf. (3.1))

$$\frac{\partial Q_x}{\partial \tau} = -\gamma\frac{\partial \rho}{\partial \eta}. \tag{3.27}$$

Finally, from (3.25) it follows that

$$\frac{\partial R_x}{\partial \tau} = Q_x. \tag{3.28}$$

Combining (3.22), (3.24), and (3.25) in $\tilde{S}_1$ we have

$$S_1 = -\sigma_x v + 2\sigma_x Q_x + \sigma_x^2 R_x + M\sigma_x' P_x, \tag{3.29}$$

with P_x, Q_x, and R_x satisfying the differential equations (3.23), (3.27), and (3.28), respectively.

To summarize, the PML equations in the absorbing "inflow" ξ-layer are

$$\frac{\partial v}{\partial \tau} + M\frac{\partial v}{\partial \xi} + \gamma\frac{\partial \rho}{\partial \eta} = -\sigma_x v + 2\sigma_x Q_x + \sigma_x^2 R_x + M\sigma_x' P_x, \tag{3.30}$$

$$\frac{\partial u}{\partial \tau} + \frac{\partial \rho}{\partial \xi} - \frac{M}{\gamma}\frac{\partial v}{\partial \eta} = -\sigma_x u, \tag{3.31}$$

$$\frac{\partial \rho}{\partial \tau} + \frac{\partial u}{\partial \xi} + \frac{1}{\gamma}\frac{\partial v}{\partial \eta} = -\sigma_x \rho, \tag{3.32}$$

$$\frac{\partial Q_x}{\partial \tau} = -\gamma\frac{\partial \rho}{\partial \eta}, \tag{3.33}$$

$$\frac{\partial P_x}{\partial \tau} = v - \sigma_x P_x, \tag{3.34}$$

$$\frac{\partial R_x}{\partial \tau} = Q_x. \tag{3.35}$$

Note that from a computational point of view (3.33)–(3.35) hardly add to the amount of computing. The quantity $\partial\rho/\partial\eta$ is evaluated in (3.30) and thus (3.33)–(3.35) weigh as three additional ODEs rather than three additional PDEs. Transforming the system (3.30)–(3.35) back to the physical space (x, y, t) yields

$$
\begin{aligned}
\frac{\partial v}{\partial t} + M\frac{\partial v}{\partial x} + \frac{\partial \rho}{\partial y} &= -\sigma_x v + 2\sigma_x Q_x + \sigma_x^2 R_x + M\sigma_x' P_x, \\
\frac{\partial u}{\partial t} + M\frac{\partial u}{\partial x} + \frac{\partial \rho}{\partial x} &= -\sigma_x u - \sigma_x M\rho, \\
\frac{\partial \rho}{\partial t} + M\frac{\partial \rho}{\partial x} + \frac{\partial u}{\partial x} + \frac{\partial v}{\partial y} &= -\sigma_x \rho - \sigma_x Mu, \\
\frac{\partial Q_x}{\partial t} &= -\gamma^2\frac{\partial \rho}{\partial y}, \\
\frac{\partial P_x}{\partial t} &= \gamma^2(v - \sigma P_x), \\
\frac{\partial R_x}{\partial t} &= \gamma^2 Q_x.
\end{aligned}
\tag{3.36}
$$

Let us briefly consider the issue of well-posedness of this new set of equations. Clearly, since the equations for P_x and R_x are ODEs these have no effect on the issue of well-posedness. The equation for Q_x, however, may affect the well-posedness of the original set of equations.

To address this question we focus the attention on the Cauchy problem and introduce the spatial Fourier transform of q as

$$
q(x, y, t) = \int_{-\infty}^{\infty}\int_{-\infty}^{\infty} \hat{q}(k_x, k_y, t)e^{i(k_x x + k_y y)}\, dk_x\, dk_y,
$$

where $\hat{q} = [\hat{v}, \hat{u}, \hat{\rho}]^T$ represents the Fourier coefficients of the field components.

Considering the initial conditions $\hat{q}(0) = [\hat{u}_0, \hat{v}_0, \hat{\rho}_0]^T$, the solution to (2.4)–(2.6) is given as

$$
\hat{q}(t) = ae^{-i(Mk_x - \nu)t} + be^{-i(Mk_x + \nu)t} + ce^{-iMk_x t},
$$

with the three vectors $a = [a_u, a_v, a_\rho]^T$, $b = [b_u, b_v, b_\rho]^T$, and $c = [c_u, c_v, c_\rho]^T$ having the entries

$$
a = \frac{\mu - \hat{\rho}_0\nu}{2\nu^2}\begin{bmatrix} k_x \\ k_y \\ -\nu \end{bmatrix}, \qquad b = \frac{\mu + \hat{\rho}_0\nu}{2\nu^2}\begin{bmatrix} k_x \\ k_y \\ \nu \end{bmatrix}, \qquad c = \frac{1}{\nu^2}\begin{bmatrix} \hat{u}_0\nu^2 - k_x\mu \\ \hat{v}_0\nu^2 - k_y\mu \\ 0 \end{bmatrix},
$$

and

$$
\nu = \sqrt{k_x^2 + k_y^2}, \qquad \mu = \hat{u}_0 k_x + \hat{v}_0 k_y.
$$

We immediately recognize the three types of waves, inherent in the linearized Euler equations, giving rise to three different wave speeds. Moreover, we note that a and b as well as c are bounded for all values of k_x and k_y confirming the strong well-posedness of the initial value problem.

Integrating the equation of Q_x yields

$$\begin{aligned}\hat{Q}_x(t) &- \hat{Q}_x(0)\\ &= i\gamma^2 a_\upsilon \frac{2\nu}{Mk_x-\nu}\sin\left[\frac{Mk_x-\nu}{2}t\right]e^{-i\frac{Mk_x-\nu}{2}t} - i\gamma^2 b_\upsilon \frac{2\nu}{Mk_x+\nu}\sin\left[\frac{Mk_x+\nu}{2}t\right]e^{-i\frac{Mk_x+\nu}{2}t},\end{aligned}$$

from which we immediately see that $\hat{Q}_x(t)$ remains bounded for all values of k_x and k_y since a_υ and b_υ are bounded, thereby establishing strong well-posedness of the system (3.36).

It should be noted that the system remains well-posed because the auxiliary equations contain spatial derivatives of the density only. Had the equations contained spatial derivatives of the velocity components strong well-posedness would have been lost. Following the general analysis outlined in [12] it follows that loss of strong well-posedness happens as a direct consequence of the nonzero term related to the vorticity wave.

Let us now briefly consider the situation where we wish to construct the PML equations in the right absorbing x-layer, $L_x \le x \le L_x + \delta_x$ ($1 \le \xi \le 1 + \delta_x$ by normalization) as illustrated in Fig. 1. We have already established that this layer is entered by a vorticity wave (with $\lambda = \lambda_0 = \frac{1}{M}$) as well as a rightward propagating acoustic wave ($\lambda = A$). The ansatz for these two waves (which are analogous to the one given in (3.1)) is

$$\begin{pmatrix} \upsilon \\ u \\ \rho \end{pmatrix}_{\lambda=\lambda_0} = \begin{bmatrix} (1+g)M \\ -(1+f)\frac{M^2 B}{\gamma} \\ 0 \end{bmatrix} e^{i\omega(\tau - \frac{1}{M}\xi - B\eta)} e^{-\frac{1}{M}\int_1^{\xi>0}\sigma(z)dz}, \tag{3.37}$$

and

$$\begin{pmatrix} \upsilon \\ u \\ \rho \end{pmatrix}_{\lambda=A} = \begin{bmatrix} (1+g)B\gamma \\ (1+f)(A-M) \\ (1+h)(1-MA) \end{bmatrix} e^{i\omega(\tau - A\xi - B\eta)} e^{-A\int_1^{\xi>0}\sigma(z)dz}. \tag{3.38}$$

It should be pointed out that we must in general consider an ansatz which is an arbitrary linear combination of the families of solutions put forward in (3.37) and (3.38). However, a substitution verifies that (3.37) and (3.38) individually are solutions to the system (3.30)–(3.35) and, as a direct consequence of linearity, so is any linear combination of (3.37) and (3.38). Thus we have the same set of PML equations in both the "inflow" and "outflow" absorbing ξ-layers, given by the system (3.36).

3.2. *The η-Layers*

Let us now direct the attention to the formulation of absorbing layers within the y-layers—see Fig. 1. In the stretched coordinate system, Eqs. (2.12)–(2.14) takes the general form

$$W_t + GW_\xi + HW_\eta = 0, \tag{3.39a}$$

where

$$W = \begin{pmatrix} v \\ u \\ \rho \end{pmatrix}, \qquad G = \begin{pmatrix} M & 0 & 0 \\ 0 & 0 & 1 \\ 0 & 1 & 0 \end{pmatrix}, \qquad H = \begin{pmatrix} 0 & 0 & \gamma \\ -\frac{M}{\gamma} & 0 & 0 \\ \frac{1}{\gamma} & 0 & 0 \end{pmatrix}. \tag{3.39b}$$

The eigenvalues of G are $(M, \pm 1)$, while H has only two nonzero eigenvalues, namely ± 1. Since $M > 0$ we have, in the ξ direction, one left-going wave and two right-going waves. For this situation one should match two waves at the right ξ-layer and one wave at the left ξ-layer. Indeed this is what was done in Subsection 3.1.

On the other hand since H has only 2 nonzero eigenvalues (± 1), it is enough to match one wave at each η-layer. By analogy to (2.15) we seek a plane of the form

$$\begin{pmatrix} v \\ u \\ \rho \end{pmatrix} = \begin{pmatrix} p_1 \\ p_2 \\ p_3 \end{pmatrix} e^{i\omega(\tau - A\xi - \mu\eta)}. \tag{3.40}$$

We find, unlike the case of (2.15), that the solvability eigenvalue, μ, has only 2 values (not three), namely

$$\mu_1 = \sqrt{1 - A^2} = B, \tag{3.41}$$

$$\mu_2 = -\sqrt{1 - A^2} = -B. \tag{3.42}$$

The corresponding eigenvectors are

$$\mathbf{p}_1 = \begin{pmatrix} B\gamma \\ A - M \\ 1 - MA \end{pmatrix}, \tag{3.43a}$$

$$\mathbf{p}_2 = \begin{pmatrix} -B\gamma \\ A - M \\ 1 - MA \end{pmatrix}. \tag{3.43b}$$

Using the methodology of (3.1) the ansatz in the η-layer takes the form

$$\begin{bmatrix} v \\ u \\ \rho \end{bmatrix} = \begin{bmatrix} \gamma B \\ \left(1 + \frac{\sigma_y}{i\omega}\right)(A - M) \\ \left(1 + \frac{\sigma_y}{i\omega}\right)(1 - MA) \end{bmatrix} e^{i\omega(\tau - A\xi - B\eta)} e^{-B\int_0^\eta \sigma_y(z)dz}. \tag{3.44}$$

In a way analogous to that utilized for deriving (3.30)–(3.35), one can then derive a set of

PML equations for both the upper and lower η-layers of the form

$$\frac{\partial v}{\partial \tau} + M\frac{\partial v}{\partial \xi} + \gamma\frac{\partial \rho}{\partial \eta} = 2\sigma_y Q_y + \sigma_y^2 R_y + \gamma\sigma_y' P_y, \tag{3.45}$$

$$\frac{\partial u}{\partial \tau} + \frac{\partial \rho}{\partial \xi} - \frac{M}{\gamma}\frac{\partial v}{\partial \eta} = 0, \tag{3.46}$$

$$\frac{\partial \rho}{\partial \tau} + \frac{\partial u}{\partial \xi} + \frac{1}{\gamma}\frac{\partial v}{\partial \eta} = 0, \tag{3.47}$$

$$\frac{\partial Q_y}{\partial \tau} = \gamma\frac{\partial \rho}{\partial \eta} - 2\sigma Q_y - \sigma^2 R_y - \sigma_y' P_y, \tag{3.48}$$

$$\frac{\partial P_y}{\partial \tau} = (\rho - \sigma P_y), \tag{3.49}$$

$$\frac{\partial R_y}{\partial \tau} = Q_y. \tag{3.50}$$

In the (x, y, t)-space the system (3.44)–(3.48) is

$$\begin{aligned}
\frac{\partial v}{\partial t} + M\frac{\partial v}{\partial x} + \frac{\partial \rho}{\partial y} &= 2\sigma_y Q_y + \sigma_y^2 R_y + \sigma_y' P_y,\\
\frac{\partial u}{\partial t} + M\frac{\partial u}{\partial x} + \frac{\partial \rho}{\partial x} &= 0,\\
\frac{\partial \rho}{\partial t} + M\frac{\partial \rho}{\partial x} + \frac{\partial u}{\partial x} + \frac{\partial v}{\partial y} &= 0,\\
\frac{\partial Q_y}{\partial t} &= \gamma^2\left[\frac{\partial \rho}{\partial y} - 2\sigma_y Q_y - \sigma_y^2 R_y - \sigma_y' P_y\right],\\
\frac{\partial P_y}{\partial t} &= \gamma^2[\rho - \sigma_y P_y],\\
\frac{\partial R_y}{\partial t} &= \gamma^2 Q_y.
\end{aligned} \tag{3.51}$$

Well-posedness of this system follows directly from the observation that only spatial derivatives of the density are introduced which, as we saw for the system (3.36) for the ξ-layer, does not affect well-posedness.

4. COMPUTATIONAL TESTS

To confirm the theoretical analysis put forward in the previous sections and study the efficiency of this new PML method, we have implemented the scheme on an equidistant grid using a 4th order centered finite-difference scheme with 3rd order closure for stability in space, while we use a 4th order Runge–Kutta scheme for advancing the equations in time. The time step, Δt, is chosen to be well below the stability limit. Contrary to the scheme proposed in [11], there is no need for applying a filter to maintain stability and, to emphasize this point, we have not used any filters in the present work.

The full set of PML equations are given as

$$
\begin{aligned}
&\frac{\partial v}{\partial t} + M\frac{\partial v}{\partial x} + \frac{\partial \rho}{\partial y} \\
&\quad = -\sigma_x v + 2\sigma_x Q_x + \sigma_x^2 R_x + M\sigma_x' P_x + 2\sigma_y Q_y + \sigma_y^2 R_y + \sigma_y' P_y - \varepsilon_x v + 2\mu_y Q_y, \\
&\frac{\partial u}{\partial t} + M\frac{\partial u}{\partial x} + \frac{\partial \rho}{\partial x} = -\sigma_x u - \sigma_x M\rho - \mu_y u, \\
&\frac{\partial \rho}{\partial t} + M\frac{\partial \rho}{\partial x} + \frac{\partial u}{\partial x} + \frac{\partial v}{\partial y} = -\sigma_x \rho - \sigma_x M u - \mu_y \rho, \\
&\frac{\partial Q_x}{\partial t} = -\gamma^2 \frac{\partial \rho}{\partial y}, \\
&\frac{\partial Q_y}{\partial t} = \gamma^2 \left[\frac{\partial \rho}{\partial y} - 2\sigma_y Q_y - \sigma_y^2 R_y - \sigma_y' P_y + \sigma_x v - 2\sigma_x Q_x \right. \\
&\qquad \left. - \sigma_x^2 R_x - M\sigma_x' P_x + \mu_x v - 2\mu_y Q_y \right], \\
&\frac{\partial P_x}{\partial t} = \gamma^2[v - \sigma_x P_x - \varepsilon_x P_x], \qquad \frac{\partial P_y}{\partial t} = \gamma^2[\rho - \sigma_y P_y], \\
&\frac{\partial R_x}{\partial t} = \gamma^2[Q_x - \mu_x R_x], \qquad \frac{\partial R_y}{\partial t} = \gamma^2[Q_y - \mu_y R_y],
\end{aligned}
\tag{4.1}
$$

as obtained by adding the two individual PML schemes derived in each of the two layers. To rigorously justify this approach one needs to do a complete analysis of the coupled system of PML equations within the corner. Unfortunately, due to the complexity of the system of equations, we have been unable to complete such an analysis and can simply conjecture that the corners also are perfectly matched. However, as we shall see shortly, the validity of this conjecture is indeed supported by the computational results.

A close inspection of the full set of PML equations, Eq. (4.1), will reveal that a few more terms, containing the profiles $\mu_{x,y}$ and ε_x, than one would obtain by simply combining Eqs. (3.36) and (3.51) have been introduced in the equations for v, u, ρ as well as Q_y, P_x, R_x, and R_y.

To understand the need for these terms and their effect, let us for simplicity consider the equations for the x-layer, (3.36), only and imagine a situation where the spatial variation of the solution is limited. It should be emphasized that this latter assumption is done solely to simpify the analysis and expose the problem. As examples of relavant scenarios where such conditions can evolve one can think of local areas of the computational domain where only little activity is present or a problem where a compact pulse has left the computational domain, leaving behind only errors caused by the numerical approximation.

Neglecting the equations for ρ and u, as they are decoupled and do not cause any problems, we recover the following system of ODEs

$$
\begin{aligned}
&\frac{\partial v}{\partial t} = -\sigma_x v + 2\sigma_x Q_x + \sigma_x^2 R_x + M\sigma_x' P_x, \\
&\frac{\partial Q_x}{\partial t} = 0, \qquad \frac{\partial P_x}{\partial t} = \gamma^2(v - \sigma_x P_x), \qquad \frac{\partial R_x}{\partial t} = \gamma^2 Q_x.
\end{aligned}
$$

The first two eigenvalues of this system are easily found to be $\lambda_{1,2} = 0$ while the remaining two are found as the solution to the equation

$$\lambda^2 + \sigma_x(1+\gamma^2)\lambda + \gamma^2\left(\sigma_x^2 - M\sigma_x'\right) = 0.$$

To guarantee that this equation has solutions with purely negative real parts, one easily reaches the condition that $\sigma_x^2 - M\sigma_x' \geq 0$, which, for $M > 0$, is always violated considering that σ_x in general is a polynomial that vanishes at the vacuum/layer interface.

As if this were not enough of a source of trouble, one may also realize that the multiple eigenvalue, $\lambda_{1,2}$, is degenerate, i.e., it has only one eigenvector. Hence, the general solution to the above systen takes the form

$$q(t) = A + Bt + Ce^{\lambda_3 t} + De^{\lambda_4 t},$$

where $q(t)$ signifies any of the 4 variables; the constants, (A, B, C, D), depend on the initial conditions; and we recall that either λ_3 or λ_4 is positive in parts of the PML layer, hence allowing for exponential growth.

The low order terms introduced in the PML to ensure absorption introduce a forcing, i.e., if the computations require very long time integration this forcing may be a source of a significant problem. As a note, we recall that this growth does not contradict the strong well-posedness established in the previous section. Indeed, strong well-posedness simply implies that the solution can be uniformly bounded by the initial conditions up to exponential growth in time.

To remove the instability, or rather unphysical growth in the PML layer, one must recall that the growth is a result of positive eigenvalues of the system as well as a Jordan block structure in the system of ODEs. One way of overcoming this problem is to attempt to shift the positive eigenvalue into the negative half plane and break the Jordan block by splitting the multiple eigenvalue.

Let us hence consider the modified system of ODEs

$$\frac{\partial v}{\partial t} = -\sigma_x v + 2\sigma_x Q_x + \sigma_x^2 R_x + M\sigma_x' P_x - \varepsilon_x v,$$
$$\frac{\partial Q_x}{\partial t} = 0, \qquad \frac{\partial P_x}{\partial t} = \gamma^2(v - \sigma_x P_x - \varepsilon_x P_x), \qquad \frac{\partial R_x}{\partial t} = \gamma^2(Q_x - \mu_x R_x),$$

where we now aim at specifying μ_x and ε_x in order to remove the growth.

The eigenvalues of this slightly modified system is easily found as $\lambda_1 = 0$, $\lambda_2 = -\gamma^2\mu_x$ while the remaining two eigenvalues are found as the solution to the equation

$$\lambda^2 + (\sigma_x + \varepsilon_x)(1+\gamma^2)\lambda + \gamma^2\left((\sigma_x+\varepsilon_x)^2 - M\sigma_x'\right) = 0,$$

which, using the results discussed above, immediately yields the condition for decay as $(\sigma_x + \varepsilon_x)^2 - M\sigma_x' \geq 0$, a sufficient condition for this being that $\varepsilon_x \geq \sqrt{|M\sigma_x'|}$.

The modifications for the equations in the y-layer are derived following a similar line of analysis and are in fact easier as only algebraic growth is appearing.

The existence of this instability, or rather growth as a result of the low order terms introduced by the PML construction, is not special to the schemes given by Eqs. (3.36) and (3.51) but is rather shared with all other known PML schemes suitable for aero-acoustics as well as electromagnetics. We shall not discuss this problem further here but rather refer to [14] where a more thorough discussion of this phenomena will be presented.

Before we consider the performance of (4.1), let us note that while the additional terms stabilize the schemes they also have the effect that the system is no longer truly a PML scheme. Even though the layers remain matched provided only that μ_x, ε_x, and μ_y are tapered in a fashion similar to σ_x and σ_y we can no longer guarantee that waves of all frequencies impinging at all angles are absorbed equally well by the layers. However, as we shall see shortly, the performance of the layers is very promising.

We shall study the performance of the PML scheme when solving (2.4)–(2.6) subject to the following continuous forcing

$$\begin{aligned}
\rho^f(x, y, t) &= e^{-(\ln 2)\frac{(x-x_a)^2+(y-y_a)^2}{\delta_a^2}} \sin\left[\frac{\pi}{10}t\right], \\
u^f(x, y, t) &= 0.05(y - y_b)e^{-(\ln 2)\frac{(x-x_b)^2+(y-y_b)^2}{\delta_b^2}} \sin\left[\frac{\pi}{10}t\right], \\
v^f(x, y, t) &= -0.05(x - x_b)e^{-(\ln 2)\frac{(x-x_b)^2+(y-y_b)^2}{\delta_b^2}} \sin\left[\frac{\pi}{10}t\right],
\end{aligned} \tag{4.2}$$

where (x_a, y_a) signifies the center of sound source of width δ_a, while (x_b, y_b) refers to the center of a vorticity source of width δ_b. The three forcing terms, Eqs. (4.2), are simply added to (2.4)–(2.6).

The profiles, $\sigma_x(x)$ and $\sigma_y(y)$, required in (4.1), are chosen as

$$\begin{aligned}
\sigma_x(x) &= \begin{cases} 0, & |x| \le L_x \\ C_x\left(\frac{|x-L_x|}{\delta_x}\right)^n, & L_x < |x| < L_x + \delta_x \end{cases}, \\
\sigma_y(y) &= \begin{cases} 0, & |y| \le L_y \\ C_y\left(\frac{|y-L_y|}{\delta_y}\right)^n, & L_y < |y| < L_y + \delta_y. \end{cases}
\end{aligned} \tag{4.3}$$

Here we assume that the computational domain is bounded by $|x| \le L_x$ and $|y| \le L_y$ while δ_x and δ_y refer to the width of the absorbing layers along x and y, respectively. The constants, C_x, C_y, and n, control the strength of the layer and we have chosen these parameters as $C_x = C_y = 1$ and $n = 4$. It should noted that no effort has been made to optimize these parameters at this point in time as the primary goal of the present work is to present a general mathematical tool for the derivation of PML methods rather than a very specific and optimized PML method. The auxiliary equations in (4.1) are advanced in time using the same scheme and time-step as for the Euler equations themselves.

The additional profiles, introduced to stabilize the PML scheme, are generally taken as

$$\varepsilon_x(x) = \sqrt{M|\sigma_x'(x)|}, \qquad \mu_x(x) = \sigma_x(x), \qquad \mu_y(y) = \sigma_y(y).$$

It should be noted that only in cases where the very long behavior is studied do we need to take $\mu_{x,y} \neq 0$.

We consider the problem in the computational domain $(x, y) \in [-50, 50]^2$ with the absorbing layers outside and position the acoustic pulse at $(x_a, y_a) = (-25, 0)$ with a width

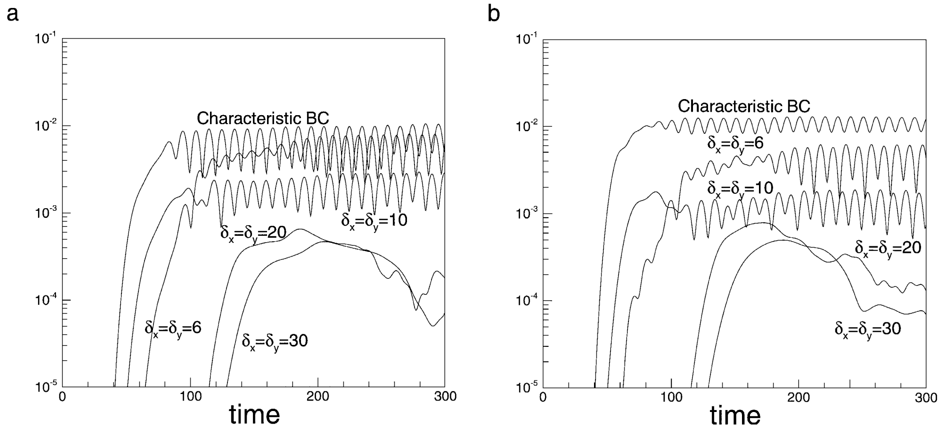

FIG. 2. The evolution of the L_2-error along the line $x = -48$ for various layer thicknesses, $\delta_x = \delta_y$ for $M = 0.5$. (a) The error on the perturbation density ρ; (b) the error on the perturbation of the velocity component v. The error computed using only characteristic boundary conditions is given for comparison.

of $\delta_a = 3$ while the vorticity pulse is positioned at $(x_b, y_b) = (25, 0)$ with a width of $\delta_b = 4$. The absorbing layers are terminated using characteristic boundary conditions.

Although an exact solution exists to this problem we have chosen to compare it to a numerical solution obtained in the domain of $(x, y) \in [-150, 150]$. It is easy to see that for $t < 317$ no reflections from the outer boundary will have sufficient time to propagate back and interact with the solution within $[-50, 50]$ and we can claim that such a solution represents the true numerical solution in an infinite domain for all $t < 317$. By using this solution as a reference rather than the exact solution we obtain a true measure of the efficiency of the PML scheme as the inherent truncation errors of the scheme approximating the equations are eliminated.

In Fig. 2 we show the L_2-error of ρ and v computed along the line $x = -48$ and $y \in [-50, 50]$, i.e., it measures the efficiency of the PML scheme in the inflow layer.

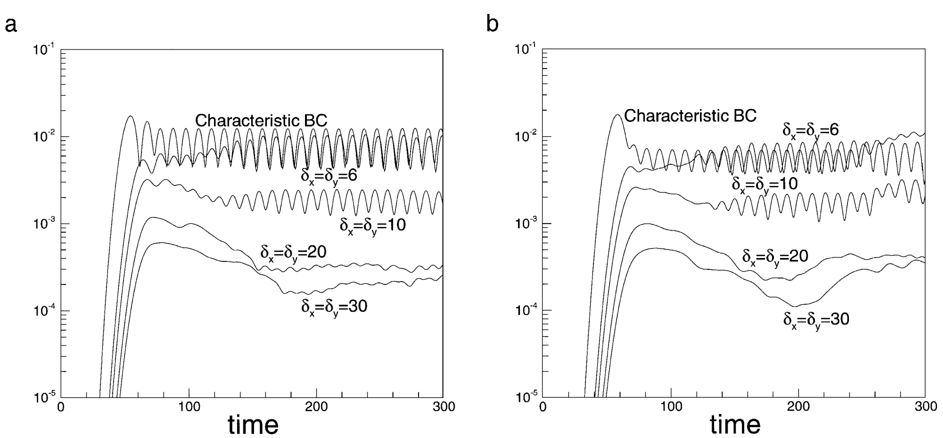

FIG. 3. The evolution of the L_2-error along the line $x = 48$ for various layer thicknesses, $\delta_x = \delta_y$ for $M = 0.5$. (a) The error on the perturbation density ρ; (b) the error on the perturbation of the velocity component v. The error computed using only characteristic boundary conditions is given for comparison.

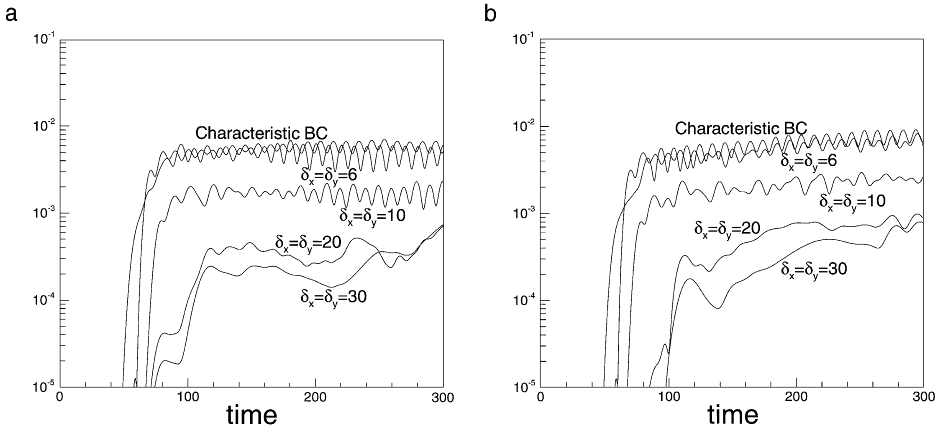

FIG. 4. The evolution of the L_2-error along the line $y = 48$ for various layer thicknesses, $\delta_x = \delta_y$ for $M = 0.5$. (a) The error on the perturbation density ρ; (b) the error on the perturbation of the velocity component v. The error computed using only characteristic boundary conditions is given for comparison.

Computing the reflection for various values of the thickness of the PML layer we clearly see how the accuracy of the computed solution is markedly increased over that arrived at using only characteristic variables. Indeed, using a layer as thin as 6 cells yields an accuracy comparable to that of the characteristic treatment while increasing the thickness improves the accuracy by close to 2 orders of magnitude.

In Fig. 3 we show a similar comparison, however, for a location near the outflow with the L_2-error being measured along the line $x = 48$ and $y \in [-50, 50]$. As in the inflow case, a layer thickness of only 6 cells yields an accuracy comparable to that of characteristics while increasing the thickness slightly has a marked effect of the overall accuracy.

A very similar conclusion can be reached for the performance of the layer in the y-direction as illustrated in Fig. 4 where we show the L_2-error along the line of $y = 48$ and $x \in [-50, 50]$. As in the direction of the flow, the performance of the PML scheme is far superior to that of using only characteristic variables.

Although we have only shown results here for $M = 0.5$, numerous computations confirm that similar conclusions can be reached for the whole subsonic range with only a very slight decay in performance as M approaches the transonic limit.

5. A FEW REMARKS

The development of efficient and accurate absorbing boundary conditions for problems in acoustics and beyond remains a very significant challenge. What we have presented here, however, provides a mathematical framework in which such development may be successful. Indeed, the development of a PML for the three-dimensional equations of acoustics is straightforward provided only that the mean flow can be considered spatially constant.

In cases where the mean flow is not aligned one may be able to apply a rotation to the problem such that the mean flow is aligned with the computational grid, thus creating a situation in which the current method is applicable. However, for the general situation where the mean flow is not aligned with one of the axes the difficulty arises due to the critical use of a special variable transformation in the development of the PML method. The identification of such a transformation in the case of a general flow would allow for the development of PML schemes for such situations using the techniques outlined in the previous sections. At this point in time we are, however, unaware of such a general transformation.

Of equal importance is the development of PML methods for problems involving smoothly varying mean flows, as in boundary layers and jets. While the mathematical tools developed so far certainly are applicable for sufficiently smooth variations, new developments are most likely needed to address the general variable coefficient problem.

ACKNOWLEDGMENT

This work was partially supported by AFOSR Grant F49620-96-1-0426.

REFERENCES

1. B. Engquist and A. Majda, Absorbing boundary conditions for the numerical simulation of waves, *Math. Comp.* **31**, 629 (1977).
2. A. Bayliss and E. Turkel, Radiation boundary conditions for wave-like equations, *Comm. Pure Appl. Math.* **33**, 707 (1980).
3. D. Givoli, Non-reflecting boundary conditions, *J. Comput. Phys.* **94**, 1 (1991).
4. S. V. Tsynkov, Numerical solution of problems on unbounded domains: A review, *Appl. Numer. Math.* **27**, 465 (1998).
5. J.-P. Berenger, A perfectly matched layer for the absorption of electromagnetic waves, *J. Comput. Phys.* **114**, 185 (1994).
6. S. Abarbanel and D. Gottlieb, A mathematical analysis of the PML method, *J. Comput. Phys.* **134**, 357 (1997).
7. L. Zhao and A. C. Cangellaris, A general approach for the development of unsplit-field time-domain implementations of perfectly matched layers for FD-TD grid truncation, *IEEE Microwave Guided Wave Lett.* **6**, 209 (1996).
8. R. W. Ziolkowski, Time-derivative Lorentz-material model based absorbing boundary conditions, *IEEE Trans. Antennas Propagat.* **45**, 656 (1997).
9. A. Taflove (Ed.), *Advances in Computational Electrodynamics* (Artech House, Boston, 1998).
10. S. Abarbanel and D. Gottlieb, On the construction and analysis of absorbing layers in CEM, *Appl. Numer. Math.* **27**, 331 (1998).
11. F. Q. Hu, On absorbing boundary conditions for linearized Euler equations by a perfectly matched layer, *J. Comput. Phys.* **129**, 201 (1996).
12. J. S. Hesthaven, On the analysis and construction of perfectly matched layers for the linearized Euler equations, *J. Comput. Phys.* **142**, 129 (1998).
13. C. K. W. Tam, L. Auriault, and F. Cambuli, Perfectly matched layers as an absorbing boundary condition for the linearized Euler equations in open and ducted domains, *J. Comput. Phys.* **144**, 213 (1998).
14. S. Abarbanel, D. Gottlieb, and J. S. Hesthaven, On long time instabilities of PML methods, in preparation.